Drosophila Cyclin J is a mitotically stable Cdk1 partner without essential functions

Friederike Althoff[1], Ivana Viktorinová[2], Johanna Kastl[3] and Christian F. Lehner[1,*]

[1] Institute of Zoology, University of Zurich, Zurich, Switzerland

[2] Max-Planck-Institute for Cell Biology and Genetics, Dresden, Germany

[3] Department of Biology, Molecular Genetics, University of Constance, Germany

[*] Correspondence to: Christian F. Lehner, University of Zurich, Institute of Zoology Winterthurerstrasse 190, 8057 Zurich, Switzerland, Tel.: 41 44 63 54871; FAX: 41 44 63 56820; E mail: christian.lehner@zool.uzh.ch

Key Words: *Drosophila*; Oogenesis; Meiosis; Syncytial cycles; Cyclin J, Cdk1, Cdk2

Abstract

Cyclin J is a cyclin family member that appears to have evolved before the metazoan radiation. Its evolutionary conservation argues for an important role but functional characterizations of Cyclin J have remained very limited. In *Drosophila*, Cyclin J is expressed only in females. Using transgenic *Drosophila* lines expressing Cyclin J versions with N- or C-terminal GFP extensions, we demonstrate that it is expressed exclusively in the germline. After low level expression in all nuclei within the germarium, it gets highly enriched in the germinal vesicle within the oocyte until stage 12 of oogenesis, followed by disappearance after germinal vesicle breakdown before the first meiotic division. Surprisingly, Cyclin J is not required for female fertility. Chromosome segregation during female meiosis, as well as the rapid early embryonic cell cycles after fertilization, occurs normally in the complete absence of Cyclin J. Cyclin J with EGFP fused at either N- or C terminus binds to Cdk1 and not to Cdk2. However, in contrast to the other known Cdk1 partners, the A- and B-type cyclins, Cyclin J is not degraded during mitosis.

Introduction

The first cyclin proteins were identified because of their rapid and complete disappearance during the early cleavage divisions in invertebrate embryos (Evans et al., 1983). Additional members of this eukaryotic protein family were subsequently identified and shown to function as regulatory subunits that associate with Cyclin-dependent protein kinases (Cdks) (Morgan, 2007). Various Cyclin-Cdk complexes are involved in the control of progression through the cell cycle or in other fundamental cellular processes like transcription. The originally described, rapid proteolysis during mitosis is only observed for the so-called mitotic cyclins. Based on sequence comparisons these cyclins have also been classified as A- and B-type cyclins. In *Drosophila*, as in other animal species, the mitotic cyclins bind to Cdk1 (Knoblich et al., 1994). The Cdk1 complexes are of special importance for the control of progression through mitosis. Activation of Cdk1 which depends on complex formation with mitotic cyclins results in entry into mitosis and transforms the cellular organization from interphase to metaphase architecture. Progression into anaphase and exit from mitosis requires inactivation of Cdk1 which results from ubiquitin-dependent degradation of the mitotic cyclins after activation of the Anaphase-Promoting Complex/Cyclosome (APC/C) ubiquitin ligase (Peters, 2006).

Cdk2 is involved in the control of progression into S phase (Woo and Poon, 2003). In mammalian cells, Cdk2 associates with A- and E-type cyclins. In *Drosophila*, Cyclin A-Cdk2 complexes have not been observed, while Cyclin E-Cdk2 complexes are clearly present *in vivo* (Knoblich et al., 1994; Meyer et al., 2000). This apparent difference might have evolved in the context of diversification of regulatory mechanisms controlling mitotic and endoreduplication cycles, respectively. While endoreduplication normally occurs only in very few cell types in mammals, this form of genome amplification by periodic S phases without intervening mitoses is extensively exploited during development and adult life of *Drosophila melanogaster* and many other organisms (Edgar and Orr-Weaver, 2001). *Drosophila* Cyclin E

and Cyclin A can both trigger entry into S phase (Knoblich et al., 1994; Sprenger et al., 1997) and at the same time contribute to a block to re-replication (Follette et al., 1998; Sauer et al., 1995; Weiss et al., 1998). While this blocking effect is eliminated by mitotic degradation in case of Cyclin A, Cyclin E degradation is not coupled to mitosis and involves different pathways (Hwang and Clurman, 2005; Sauer et al., 1995). In *D. melanogaster*, Cyclin E might therefore have been selected as the unique Cdk2 regulator that works for S phase regulation in both mitotic and endocycles.

In contrast to A-, B- and E-type cyclins, the role of Cyclin J has not yet been characterized in detail. Cyclin J was originally identified in a yeast two hybrid screen for *Drosophila* proteins that interact with *Drosophila* Cdk1/Cdc2 and Cdk2/Cdc2c (Finley Jr. et al., 1996). Cyclin J mRNA and protein were detected exclusively during oogenesis and early embryogenesis (Kolonin and Finley, 2000). Microinjection of antibodies against Cyclin J as well as aptamers into early *Drosophila* embryos was reported to cause severe mitotic defects. These findings are consistent with the idea that Cyclin J provides a function specifically required during the special early cycles at the start of *Drosophila* embryogenesis where progression through the cell cycle is extremely rapid, omitting gap phases and cytokinesis.

Based on its expression pattern, Cyclin J might also function during oogenesis. *Drosophila* oogenesis starts with an asymmetric division of germline stem cells at the distal end of an ovariole (for a detailed description of oogenesis see Spradling, 1993). The differentiating daughter cell, progresses through four cell division cycles with incomplete cytokinesis resulting in 16-cell clusters interconnected by ring canals. Fifteen cells of the cluster develop into nurse cells and one into an oocyte. The oocyte enters meiosis and remains arrested in a special diplotene stage with the chromatin compacted into a karyosome for most of oogenesis. The nurse cells progress through several endoreduplication cycles. Egg chambers are completed by the formation of an enveloping epithelial layer of somatic follicle cells at the proximal end of the germarium. During their travel from the distal germarium to the proximal

end of the ovariole, egg chambers progress through 14 stages during which the oocyte acquires abundant maternal stores as well as an egg shell. During stage 13, fully grown oocytes enter into the first meiotic division. After germinal vesicle breakdown and spindle formation, they arrest in metaphase of meiosis I in stage 14. Completion of meiosis occurs only after egg activation which is triggered by egg laying.

To evaluate whether *Drosophila* Cyclin J might function already during oogenesis, we have generated *Drosophila* females that completely lack this cyclin. Surprisingly, their fertility was found to be normal. Our genetic characterization demonstrates therefore that Cyclin J is not required for progression through the mitotic cycles of the germline cells at the start of oogenesis. Moreover, it is entirely dispensable for meiosis and the syncytial cycles at the onset of embryogenesis. Like the *Drosophila* A- and B-type cyclins, Cyclin J appears to associate with Cdk1 and not with Cdk2. But in contrast to the other Cdk1 partners this unusual cyclin is not degraded during mitosis.

Materials and Methods

Fly strains and genetics

P{wHy}CycJ^{DG29702}, *PBac{5HPw*$^{+}$*}CycJ*^{A138} and *Df(3L)Exel6095* which deletes *CycJ* were obtained from the Bloomington Drosophila Stock Center at Indiana University. *PBac{RB}e01160* and *PBac{XP}d0738*5 were obtained from the Exelixis Collection at the Harvard Medical School and used for the generation of *Df(3L)AJ14/TM3, Ser* as described by (Parks et al., 2004; Thibault et al., 2004). *CycE*^{01672} (Lilly and Spradling, 1996) was kindly provided by Mary Lilly (NIH, Bethesda, MD, USA). The lines with *CycA*^{C8LR1} (Sigrist and Lehner, 1997), *CycA*^{neo114} (Lehner and O'Farrell, 1989), *CycB*^{2}, *CycB*^{3}, *CycB3*^{3} (Jacobs et al., 1998), *CycE*^{AR95}, *Cyc*^{pz5} (Knoblich et al., 1994), *P{prd-GAL4}* (Brand and Perrimon, 1993), *P{matα4-GAL-VP16}V2H* (Hacker and Perrimon, 1998), *P{UAS-Cdk1-myc}III.1* or *P{UAS-Cdk2-myc}III.2* (Meyer et al., 2000) or with two *gEGFP-Mps1* transgene insertions (II.1 and II.2) resulting in expression of EGFP-Mps1 under control of the Mps1 cis-regulatory region (Fischer et al., 2004) have been described. Lines with the transgenes *gCycJ*, *gEGFP-CycJ*, *gCycJ-EGFP*, *UAS-EGFP-CycJ*, *UAS-CycJ-EGFP*, *gcal1-EGFP*, *garmi*, or *gCG14971* were obtained after P element-mediated germline transformation with the constructs described below. Selected transgene insertions were combined with *Df(3L)AJ14* by meiotic recombination. *Df(3L)AJ14, garmi III.8, gCG14971 III.10* can be kept as a homozygous stock. The presence or absence of various genes on the original *Df(3L)AJ14* chromosome and its derivatives was confirmed by PCR assays using the following gene-specific primer pairs: IV35 (5'-CGATGGTGGTTCCAAGACC-3') and IV36 (5'-GCCTGGTCTATTGATCATCG-3') for an *eIF5B* fragment, IV37 (5'-CGAGCAGCACTATTCATTCC-3') and IV38 (5'-GGAATGTTCTCCGCTTCACC-3') for an *armi* fragment, IV39 (5'-GTCGCGTCGCTTCAGCACG-3') and IV40 (5'-TTTCGCGCAGTTCATAATGCAG-3') for an *CG14971* fragment, AF22 (5'-CCTGGCTAAGACGCACTGG-3') and AF23 (5'-GCTATATGAAGACAAGTGATGG-3') for a *CycJ* fragment, XP5 (5'-

AATGATTCGCAGTGGAAGGCT-3') and RB3 (5'-TGCATTTGCCTTTCGCCTTAT-3') for the amplification of the *XP-RB* hybrid transposon.

C(1;Y), y^1 v^1 f^1 B^1: y^+/C(1)RM, y^2 su(wa)^1 w^a flies were kindly provided by Terry Orr-Weaver (Whitehead Institute for Biomedical Research, Cambridge, MA, USA). Males from this stock were used for the analysis of X chromosome non-disjunction during meiosis in oocytes as described (Kerrebrock et al., 1992). The different genotypes of the females analyzed were w^1 (for control), or *P{wHy}CycJ*^{DG29702}, or +/+; *Df(3L)AJ14, garmi III.8, gCG14971 III.10*, or *gCycJ II.41/+*; *Df(3L)AJ14, garmi III.8, gCG14971 III.10*. For these genotypes, the corrected total X non-disjunction rate (Kerrebrock et al., 1992) determined from more than 1300 progeny was found to be 0.22%, 1.07%, 0.41% and 0.44%, respectively.

For our analysis of genetic interactions between *CycJ* and *CycE*, we crossed virgin females of the genotype *Df(3L)AJ14, garmi III.8, gCG14971 III.1/Df(3L)AJ14* (*CycJ*-deficient), or *CycE*^{01672} (*CycE* hypomorph), or *CycE*^{01672}; *Df(3L)AJ14, garmi III.8, gCG14971 III.1/Df(3L)AJ14* (double mutant) with w^1 males and counted the number of progeny which was found to be 440 (+/- 40 s.d, n = 3), 135 (+/- 11 s.d, n = 3) and 127 (+/- 34 s.d, n = 2) with *CycJ*-deficient, *CycE* hypomorph and double mutant females, respectively. Genotypes and results of the experiments addressing genetic interaction between CycJ and CycA, CycB and CycB3 are provided in Supplementary Figure 1.

Plasmid constructions

The DNA fragments used for the *CycJ*, *armi* and *CG14971* transgene constructs were derived from the BACR09B04 clone (Hoskins et al., 2000). A 5 kb *Bgl*II fragment including most of *armi* was subcloned into *Bam*H1 and *Bgl*II cut pSLfa1180, resulting in cloning intermediate 1. A neighbouring 4 kb *Bgl*II fragment with the remainder of *armi*, *CycJ* and a small part of *CG14971* was subcloned into *Bgl*II cut pLitmus28, resulting in intermediate 2. The rest of *CG14971* was enzymatically amplified using the primer pair IV5 (5'-

CAATGGCCCAAGTTATCTCATTCG-3') and IV6 (5'-CCA GGCGGCCGC ACTCTGACAACTTTTTGGTGCG-3') introducing a *Not*I site. The resulting PCR product was cut with *Bgl*II and *Not*I and inserted into the corresponding sites within the intermediate 1, resulting in intermediate 3. The *CycJ* gene was deleted from intermediate 2 with an inverse PCR with the primer pair IV3 (5'-CCGA GCGGCCGC ACCCATTGAAACACGCC-3') and IV4 (5'-CGAA GCGGCCGC AGCAGCGTTCCCAGAC-3') followed by digestion with *Not*I and re-ligation, resulting in the intermediate 4. The *Bgl*II fragment from the intermediate 4 was subsequently inserted into the *Bgl*II site within the intermediate 3, resulting in intermediate 6. To arrive at the *garmi* construct, we first transferred a 2.2 kb *Sal*I-*Xba*I fragment with the 5' region of *armi* from intermediate 6 into *Xho*I and *Xba*I cut pCaSpeR4, resulting in intermediate 7. The construct was completed by transposing a 3.8 kb *Xba*I-*Not*I fragment with the 3' region of *armi* from intermediate 6 into the corresponding sites of intermediate 7. To arrive at the *gCG14971* construct, we transposed a 4.2 kb *Not* I fragment from intermediate 6 into the *Not*I site of pCaSpeR4. The *gCycJ* construct was obtained by inserting the 4 kb *Bgl*II fragment from intermediate 2 into the *Bam*HI site of pCaSpeR4. For the *gEGFP-CycJ* construct, we first subcloned a 0.5 kb *Sal*1 fragment including the translational start site from intermediate 2 into the corresponding site of pBluescript KS+ followed by introduction of an *Nhe*I site at the translational start of *CycJ* by inverse PCR using the primer pair IV48 (5'-GGCG GCTAGC ATGGAGCAGAAAGTGGCTGCC -3') and IV49 (5'-GGAG GCTAGC TGTATCGAAATTGAATGCAATGCC-3'). After inserting the EGFP coding sequence as an *Xba*I fragment into this newly created site, the modified *Sal*I fragment containing the EGFP sequence was used to replace the original *Sal*I fragment in intermediate 2, followed by transposition of the *Bgl*II fragment into the *Bam*HI site of pCaSpeR4. For the *gCycJ-EGFP* construct, an *Nhe*I site was introduced into intermediate 2 immediately upstream of the translational stop of *CycJ* by inverse PCR using the primer pair IV50 (5'-GGCG GCTAGC TAGTAAAAGGGAAAAACGAAACTATTAC -3') and IV51 (5'-

GAGG GCTAGC ATCTTTGGCTACACTCTCCACTTTG-3'). After insertion of the EGFP coding sequence as an *Xba*I fragment into this newly created site, the *Bgl*II fragment was transposed in the *Bam*HI site of pCaSpeR4 These constructs for *CycJ* expression without or with EGFP at either N- or C terminus under control of the genomic *CycJ* cis-regulatory region contain the complete intergenic regions up- and downstream from *CycJ* as well as the genomic 5' and 3' UTRs.

The *pUAST-EGFP-CycJ* construct was obtained by enzymatic amplification of the *CycJ* sequence from the *gEGFP-CycJ* construct with the primer pair JoK10 (5'-AGCTGTAC GCGGCCGC CATGGAGCAGAAAGTGGC-3') and JoK11 (5'-TTTTCC GGTACC CTAATCTTTGGCTACACTCTC-3') which introduced flanking *Not*I and *Kpn*I sites, respectively. After digestions with these enzymes, the PCR fragment was transposed into the corresponding sites within *pUAST-EGFP-MCS* (Schittenhelm et al., 2007). The *pUAST-CycJ-EGFP* construct was obtained by amplification of the *CycJ* sequence from the *gEGFP-CycJ* construct with the primer pair JoK10 and JoK12 (5'-TCCCTT GGTACC ATCTTTGGCTACACTCTCCAC-3') which also introduced flanking *Not*I and *Kpn*I sites, respectively. After digestions with these enzymes, the PCR fragment was transposed into the corresponding sites within *pUAST-MCS-EGFP* (Schittenhelm et al., 2007). The *CycJ* region in *pUAST-EGFP-CycJ* and *pUAST-CycJ-EGFP* was completely sequenced and found to be correct.

Sequence comparisons

The cyclin tree (Fig. 1) was constructed using the on-line version of T-REX (Makarenkov, 2001); www.trex.uqam.ca) based on a Clustal W alignment for which only cyclin box regions without N-terminal extensions were used in case of A-, B- and E-type cyclins. The J-type cyclins do not have an N-terminal extension preceding the cyclin box region. Accession

numbers of the used cyclin J sequences are NP_061957.2, AAH35871.3, NP_766427.1, NP_001038995.1, NP_523903.1, XP_001641369.1, XP_001237463.2, EDQ87852.1.

Immunoprecipitation, immunoblotting and immunofluorescence

Oocytes for immunoprecipitation experiments were mass isolated (Page and Orr-Weaver, 1997) from *gCycJ-EGFP II.6*, or *gEGFP-CycJ III.16*, or *gcal1-EGFP II.1*, or *gEGFP-Mps1 II.1, II.2* females before extract preparation. Embryos were collected for 3 hours on apple agar plates from crosses of *UAS-Cdk1-myc III.1*, *UAS-Cdk2-myc III.2* males with females, which were either *matα4-GAL-VP16*/*CyO* or *matα4-GAL-VP16, UAS-EGFP-CycJ II.1*/*CyO* or *matα4-GAL-VP16, UAS-CycJ-EGFP II.2*/*CyO*, and aged for 3 hours at 25°C. Immunoprecipitation from native oocyte and embryo extracts as well as protein identification by mass spectroscopy was done essentially as described (Schittenhelm et al., 2007) using affinity-purified rabbit antibodies against GFP (IS28) in combination with Protein-A-Sepharose beads (Affi-Prep, Biorad). The proteins immunoprecipitated from either ovary or embryo extracts which were analyzed by immunoblotting (Fig. 4 A or C, respectively) were isolated using an amount of extract which was 16 or 80 times more, respectively, than the amount of extract loaded for parallel analysis.

For immunoblotting, oocytes were mass isolated from *gCycJ-EGFP II.6* females before fixation in a 1:1 mixture of methanol and heptane. Fixed oocytes were transferred to a 1:1 mixture of glycerol and EB buffer (Edgar et al., 1994). After DNA labelling with Hoechst 33258 (1 μg/ml), oocytes were sorted according to their developmental stage with an inverted fluorescence microscope.

Immunoblots were probed with affinity-purified rabbit antibodies against GFP (IS28) at a dilution of 1:3000, affinity-purified rabbit antibodies against Cdk2 at 1:4000, mouse monoclonal antibodies against GFP (Roche) at 1:500, a mouse monoclonal antibody against a

PSTAIR peptide (SIGMA, P7962) at 1:50000 and a mouse monoclonal antibody against a human myc peptide (9E10) at 1:15.

For fluorescence microscopy, ovaries were dissected from *gEGFP-CycJ III.6* females as described (Page and Hawley, 2001). Oocytes were fixed for 20 minutes in 2% paraformaldehyde in phosphate buffered saline containing 0.5% Nonidet-P40. After DNA labelling with Hoechst 33258 (1 μg/ml), ovaries were analyzed with an Olympus FluoView 1000 laser scanning confocal microscope. For immunofluorescent labeling of embryos, we collected eggs for 1 hour on apple agar plates and aged at 25°C. Eggs were collected from a cross of $CycA^{C8LR1}$, *prd-GAL4/TM3, Sb P{35UZ}2* females with *UAS-CycJ-EGFP II*; $CycA^{C8LR1}$*/TM3, Ser* males and aged for 7 hours. Eggs were also collected from a cross of *Df(3L)AJ14, garmiII.8, gCG14971 III.10/Df(3L)AJ14* females with w^1 males and aged for 1 hour. Embryos were fixed essentially as described previously (Karr and Alberts, 1986). For immunofluorescent labeling we used mouse monoclonal antibody DM1A anti-α-tubulin (Sigma) at 1:8000, rabbit serum against *Drosophila* Cyclin A at 1:3000. Secondary antibodies were Cy5-conjugated goat antibodies against mouse IgG (Jackson Immunochemicals) and Alexa 568-conjugated goat antibodies against rabbit IgG (Molecular Probes). For the DNA staining of embryos, we also used Hoechst 33258 at 1 μg/ml. Embryos were analyzed with a Zeiss Cell Observer HS wide field fluorescence microscope.

Results

Cyclin J has evolved before the metazoan radiation

When originally identified in *Drosophila* (Finley Jr et al., 1996), *Cyclin J* did not appear to have homologs in other species. However, subsequent additions to Genbank have revealed that this cyclin type is not restricted to *Drosophila*. While not recognizable in plant genomes (Guo et al., 2007; Wang et al., 2004), *Cyclin J* homologs are present throughout the metazoan radiation (Fig. 1, data not shown). In the mammalian lineage, paralogous cyclin J genes (*Cyclin J* and *Cyclin J-like*) are apparent, as also in case of the better-characterized A-, B-, D- and E-type cyclins. In contrast, only single orthologs for each of these cyclin types including *Cyclin J* are present in the *Drosophila* genome. Importantly, a cyclin J homolog can also be identified in *Monosiga brevicollis*, a member of the choanoflagellates which are considered to be the closest unicellular relatives of metazoans.

The pattern of Cyclin J expression revealed by EGFP fusion transgenes

Cyclin J has evolved before the specialized syncytial cycles characteristic of early insect embryogenesis. Consistent with the known expression pattern (Finley Jr. et al., 1996; Kolonin et al., 2000), it might therefore have functions already during oogenesis and not just during the syncytial cycles where it has been characterized functionally so far. For a more detailed analysis of Cyclin J expression during oogenesis, we generated transgenic lines expressing Cyclin J fused to EGFP either at the N- or the C-terminus under the control of the genomic Cyclin J regulatory sequences. The results obtained with multiple *gEGFP-CycJ* and *gCycJ-EGFP* lines were essentially identical (Fig. 2 and data not shown).

EGFP-Cyclin J signals above background were detected in the germarium at the distal end of ovarioles. Based on the EGFP pattern in the germarium, all germline cells appeared to be weakly positive in contrast to somatic cells (Fig. 2C-E). In the newly formed egg chambers at stage 1 of oogenesis, the peripheral somatic follicle cells did definitely not display EGFP

fluorescence, while the germ line derivatives in the interior were positive (Fig. 2C-E). Signals in the oocyte were stronger than in the nurse cells. All signals were nuclear. In the oocyte, EGFP-Cyclin J was observed throughout the germinal vesicle, whereas the condensed DNA was restricted to the compact karyosome (Fig. 2I-K). After germinal vesicle break down during stage 13, we were unable to detect signals that were clearly above the uniform substantial background fluorescence (Fig. 2L-N). Similarly, after egg deposition and fertilization, we were unable to detect signals that were clearly above background (data not shown).

For further clarification whether Cyclin J is still present in oocytes after germinal vesicle breakdown, we performed immunoblotting experiments. Egg chambers were sorted microscopically before extract preparation. In extracts prepared from stage 12 egg chambers (i.e. before germinal vesicle breakdown) Cyclin J-EGFP was clearly detectable by immunoblotting with antibodies against GFP (Fig. 3, lane 3), as expected from the observed pattern of EGFP fluorescence in ovaries (Fig. 2). However, in extracts prepared from stage 14 egg chambers, Cyclin J-EGFP was essentially no longer detectable (Fig. 3, lane 4). Similar observations (data not shown) were made with extracts from females expressing EGFP-Cyclin J, although expression levels on average appeared somewhat lower with *gCycJ-EGFP* lines in comparison to *gEGFP-CycJ* lines. In extracts prepared from early embryos collected from females with either a *gEGFP-CycJ* or a *gCycJ-EGFP* transgene, we were also unable to detect the EGFP tagged Cyclin J variants (data not shown). We conclude therefore that the levels of Cyclin J fused to EGFP decrease during the final stages of oogenesis following germinal vesicle breakdown.

Cyclin J binds to Cdk1

To identify proteins that associate with Cyclin J we immunoprecipitated CycJ-EGFP from extracts prepared from ovaries of *gCycJ-EGFP* females. In control experiments, we used the

same affinity-purified antibodies against EGFP for immunoprecipitation of Cal1-EGFP from extracts prepared from ovaries of *gcal1-EGFP* females. MS/MS analysis was used to identify co-immunoprecipitated proteins. Among the proteins which were specifically co-immunoprecipitated with CycJ-EGFP, we clearly detected Cdk1 but not Cdk2 (Supplementary Table 1). Immunoblot analyses confirmed that Cdk1 but not Cdk2 was co-immunoprecipitated with CycJ-EGFP (Fig. 4A). Moreover, in a similar experiment using EGFP-Mps1 as a control, we also observed co-immunoprecipitation of Cdk1 but not Cdk2 with N-terminally EGFP tagged CycJ in immunoblot and MS/MS analyses (data not shown).

Cdk1 and Cdk2 expression levels appear to be comparable (Karsten Sauer and C.F.L., unpublished information) and both have been readily detected by shot gun proteomics (Brunner et al., 2007). Therefore, the observation that Cdk1 was co-immunoprecipitated by both EGFP-CycJ and CycJ-EGFP from ovary extracts strongly suggested that Cyclin J prefers Cdk1 over Cdk2 as partner kinase. To confirm this partner preference and circumvent the limited detection sensitivity resulting from the low expression of transgenes driven by the *CycJ* cis-regulatory region we performed experiments after overexpression in embryos. Overexpression of EGFP-Cyclin J during the embryonic cell division cycles was achieved with an appropriate UAS transgene inherited from the father in combination with maternally expressed *matα4-GAL-VP16*. Moreover, in addition to *UAS-EGFP-CycJ,* we simultaneously expressed *UAS-Cdk1-myc* and *UAS-Cdk2-myc*. The simultaneous overexpression of EGFP-Cyclin J, Cdk1-myc and Cdk2-myc did not noticeably affect embryonic development (data not shown). Immunoblotting experiments with embryonic extracts and anti-myc antibodies clearly demonstrated that Cdk1-myc and Cdk2-myc can be identified unambiguously even after co-expression because of their distinct electrophoretic mobility (Fig. 4B). Immunoblotting with anti-myc also demonstrated that Cdk1-myc and Cdk2-myc were expressed at comparable levels (Fig. 4B, data not shown). However, after immunoprecipitation with anti-EGFP, we observed only Cdk1-myc and not Cdk2-myc in the

EGFP-Cyclin J immunoprecipitates (Fig. 4C). Moreover, we also detected the endogenous untagged Cdk1 in the EGFP-Cyclin J immunoprecipitates while Cdk2 was not detectable (Fig. 4C). These results strongly support the notion that Cyclin J associates specifically with Cdk1.

Cyclin J-EGFP is not degraded during M phase

The known *Drosophila* Cdk1 partner cyclins, the A- and B-type cyclins, become rapidly degraded during mitosis (Lehner and O'Farrell, 1990). In the germarium, therefore, these mitotic cyclins are absent from cells in late mitosis and early G1 (Hatfield et al., 2005; Wang and Lin, 2005). Our observation that EGFP-Cyclin J and Cyclin J-EGFP was present at comparable levels in all germline cells within the germarium suggested that Cyclin J is not degraded during mitosis. To evaluate the behavior of Cyclin J during mitosis, we used the UAS/GAL4 system to drive its expression during embryogenesis. The developmentally controlled, highly reproducible division programme of embryogenesis facilitates careful analyses. We used *prd-GAL4* to drive expression of Cyclin J-EGFP (Fig. 5) or EGFP-Cyclin J (data not shown) in alternating epidermal stripes. Embryos were fixed at the stage of mitosis 16. Progression through mitosis 16 occurs earlier in the dorsal epidermis than in the ventral epidermis. After fixation at the stage of mitosis 16, cells in the dorsal epidermis in many embryos are already in G1 of cycle 17 while the cells in the ventral epidermis are still in G2 before mitosis 16. As each embryonic division partitions the embryo into progressively smaller cells, the nuclear density revealed by DNA staining in such embryos is twice as high in the dorsal epidermis in comparison to the ventral epidermis (Fig. 5C,F). Moreover, as previously described, the A- and B-type cyclins are degraded in mitosis 16 and remain unstable during G1 of cycle 17 (Sigrist and Lehner, 1997). Therefore, anti-Cyclin A labeling is absent from the dorsal epidermal cells and, conversely, present in the cytoplasm of ventral epidermal cells in such embryos (Fig. 5A,D). However, Cyclin J-EGFP fluorescence in the expressing epidermal stripes was not decreased in the dorsal G1 region compared to the

ventral G2 region (Fig. 5D). These observations indicate that Cyclin J is an unusual Cdk1 partner. In contrast to the other Cdk1 partners, i.e. the A- and B-type cyclins, Cyclin J does not appear to become degraded during mitosis. The absence of D- and KEN boxes from the predicted Cyclin J amino acid sequence further supports this notion. These sequence motifs are known to mediate the APC/C-dependent polyubiquitylation and consequential proteasomal degradation of A- and B-type cyclins during M and G1 phases (Peters, 2006).

prd-GAL4 driven *UAS-CycJ-EGFP* expression in *CycA* mutant embryos allowed us also to address whether Cyclin J might be able to replace Cyclin A functionally. We have previously demonstrated that the failure of epidermal cells to progress beyond G2 of cycle 16 which is caused by a loss of zygotic *CycA* function is readily prevented by *prd-GAL4* driven *UAS-CycA* expression (Reber et al., 2006). However, this premature cell cycle arrest in G2 before mitosis 16 in *CycA* mutants (Fig. 5G-I) was not prevented by analogous Cyclin J-EGFP expression (Fig. 5J-L). In both, *CycA* mutants and sibling embryos, we observed the same results after *prd-GAL4* driven expression of either *UAS-CycJ-EGFP* (Fig. 5) or *UAS-EGFP-CycJ* (data not shown).

Cyclin J is not required for oogenesis and early embryonic development

To address the function of Cyclin J, we generated lines completely lacking the *CycJ* gene. Transposon insertions carrying FRT sites allowed a Flp recombinase-mediated isolation of an 11 kb chromosomal deletion, *Df(3L)AJ14*, removing *CycJ* and the flanking genes *armitage (armi)* and *CG14971* (Fig. 6A). Characterization of the *Df(3L)AJ14* chromosome by PCR confirmed the presence of the expected deletion (Fig. 6B). To restore the function of the flanking genes, we introduced transgenes (*garmi* and *gCG14971*) carrying genomic fragments including *armi* and *CG14971*, respectively, by P element-mediated germline transformation and recombined insertions with *Df(3L)AJ14*.

Initial analyses revealed that homozygous *Df(3L)AJ14* progeny from heterozygous parents eclosed as adults. The frequency of these adults in comparison to heterozygous siblings (Table 1) indicated that the genes *CycJ, armi* and *CG14971* are completely dispensable for development to the adult stage. We also obtained normal numbers of adults homozygous for *Df(3L)AJ14* which had in addition either one or the other or both transgene insertions (*garmi III.8* and *gCG14971 III.10*). These transgene insertions therefore do no disrupt gene functions required for development to the adult stage.

Subsequent analysis of flies lacking one or several of the genes *CycJ, armi* and *CG14971* indicated that *armi* but not the other genes are required for normal fertility (Table 1). *armi* encodes a putative RNA helicase involved in the RNA interference pathway and is known to be required for normal fertility (Cook et al., 2004). Females without the *armi* gene did not produce eggs and males had a reduced fertility (Table 1). The *armi* null phenotype therefore might be more severe than the phenotypes observed previously with partial loss of function alleles which result in abnormally patterned eggs in reduced numbers (Cook et al., 2004). *CG14971* is an uncharacterized gene which appears to encode a ubiquitously expressed member of the solute carrier protein family.

Our conclusion that *CycJ* is not required for viability and fertility was further supported by our characterization of a recently isolated transposon insertion $P\{wHy\}CycJ^{DG29702}$ (Huet et al., 2002). Our sequence analysis of a PCR fragment confirmed that this insertion disrupts the *CycJ* coding sequence after the second codon. Therefore the insertion is likely to cause a complete loss of *CycJ* function. Flies homozygous or hemizygous for this insertion eclosed in normal numbers and were found to be fully fertile (Table 1). The same findings (data not shown) were also observed with flies hemizygous for $PBac\{5HPw^{+}\}CycJ^{A138}$, a transposon insertion which we also confirmed to reside in the first intron and therefore might not necessarily impair *CycJ* gene function.

To evaluate whether loss of *CycJ* might result in more subtle defects during the syncytial cycles of early embryogenesis, we collected eggs from *CycJ*-deficient females (Fig. 6C) and analyzed the frequency and appearance of mitotic figures after fixation and DNA staining. However, apart from rare abnormalities, which were also observed to the same extent in control collections, defects were not apparent (Fig.6D). Similarly, we failed to detect an increased rate of X chromosome non-disjunction during meiosis in *CycJ*-deficient females (see Materials and Methods). A double mutant analysis confirmed that Cyclin J is unlikely to have substantial functional overlap with Cyclin E. The reduced fertility of females homozygous for the hypomorphic mutation $CycE^{01672}$ (Lilly and Spradling, 1996) was marginally enhanced in double mutants lacking *CycJ* function completely (see Materials and Methods). Moreover, additional attempts to detect potential genetic interactions between *CycJ* and *CycA*, *CycB*, *CycB3* or *CycE* equally failed to reveal clear evidence for functional redundancies (Supplementary Figure 1). *CycJ*-deficient females with only one functional gene copy of *CycA*, *CycB*, *CycB3* or *CycE* had a very similar fertility as those with two functional copies. In addition, progression through the syncytial cycles was not compromised by reducing the number of functional copies of these other cyclin genes in *CycJ*-deficient mothers.

Discussion

Sequence comparisons demonstrate that Cyclin J is an evolutionary conserved cyclin family member. *Cyclin J* homologs are present throughout the metazoan radiation, as well as in their unicellular sister group. While this evolutionary conservation points to an important role of Cyclin J, its functional characterization has remained very limited. Moreover, our analyses contradict previous conclusions and reveal a number of unexpected findings. Using transgenic *Drosophila* lines expressing Cyclin J versions with N- or C-terminal GFP extensions, we demonstrate that it binds to Cdk1 and not to Cdk2. However, in contrast to the other known Cdk1 partners, the A- and B-type cyclins, Cyclin J does not appear to become proteolysed during mitosis. In addition, its expression pattern is far more restricted. While A- and B-type cyclin expression is observed in all mitotically proliferating and meiotic cells, Cyclin J is only expressed in the female germ line. While initially present at low levels in all nuclei within the germarium, it gets highly enriched in the germinal vesicle within the oocyte during egg chamber development until stage 12, and disappears again later concomitant with germinal vesicle breakdown at the start of the first meiotic division. Surprisingly, we find that Cyclin J is not required for female fertility. Chromosome segregation during female meiosis as well as the rapid early embryonic cell cycles after fertilization occurs normally in the complete absence of Cyclin J. Only a slight increase in the number of embryos that do not develop beyond cycle 1 is noticeable when averaging over many collections from *CycJ*-deficient females.

Most of our results are at variance with those published earlier (Finley Jr. and Brent, 1994; Kolonin and Finley, 2000). Based on the described yeast two hybrid and co-immunoprecipitation experiments, *Drosophila* Cyclin J for instance was suggested to prefer Cdk2 over Cdk1 as a partner kinase. Curiously, in these same yeast two hybrid experiments, *Drosophila* Cyclin E was also observed to have the opposite preference from what we have observed *in vivo* (Finley Jr. and Brent, 1994; Knoblich et al., 1994). In case of the published

co-immunoprecipitation experiments (Kolonin and Finley, 2000), a cross reaction of the affinity-purified rabbit antibodies against Cyclin J with a protein of similar molecular might have compromised the validity of these earlier conclusions. Concerning the validity of our present discordant conclusions, we emphasize that we cannot exclude the possibility that the EGFP fusions, which we have studied, do not behave like the untagged endogenous Cyclin J. We consider this possibility to be unlikely, as we have obtained consistent results with EGFP fused at either the N- or the C-terminus of Cyclin J. Moreover, experiments with other cyclins have clearly demonstrated that EGFP extensions do not affect their function (Buszczak et al., 2007; den Elzen and Pines, 2001; Hagting et al., 1998; Jackman et al., 2002). Finally, our finding that progression through the syncytial cycles of early *Drosophila* embryogenesis is not noticeably affected by the complete absence of Cyclin J is entirely independent of assumptions concerning the functionality of our Cyclin J fusions. The severe mitotic defects reported to occur after injection of antibodies or aptamers against Cyclin J (Kolonin and Finley, 2000) might reflect cross-reactions or indicate that the binding of these reagents to Cyclin J has other consequences than eliminating Cyclin J altogether.

The absence of obvious phenotypic abnormalities after complete elimination of *CycJ* function might indicate functional redundancies. Our preliminary evidence argues against the suggestion that it is the function of Cyclin A, B, B3 or E which masks a Cyclin J requirement. Our failure to prevent the characteristic *CycA* zygotic effect mutant phenotype by expression of Cyclin J fusions with EGFP in embryos argues against major functional overlap between Cyclin A and Cyclin J. In addition, a reduction of the number of functional *CycA, CycB, CycB3* or *CycE* gene copies in *CycJ*-deficient females using multiple strong or null alleles did not consistently reduce their fertility or affect progression through the syncytial cycles in progeny. Moreover, genetic elimination of *CycJ* in females with reduced *CycE* function did not further reduce their compromised fertility. Future unbiased genetic screens in our *CycJ*-

deficient background might lead to an identification of components acting redundantly with Cyclin J.

Redundant functional pathways might also explain that some metazoans like *C. elegans* appear to have lost Cyclin J and that the expression pattern of Cyclin J varies in different metazoan lineages. In contrast to *Drosophila* Cyclin J, which appears to be expressed exclusively in the female germline, the human Cyclin J paralogs are much more widely expressed in various somatic tissues according to the tissue distribution of the expressed sequence tags. The apparent somatic expression in humans, as well as the presence of a Cyclin J homolog in the choanoflagellate *Monosiga brevicollis*, clearly argues against the notion that the primordial Cyclin J function is oogenesis-specific.

Acknowledgements

We thank Anja Katzemich, Brigitte Jaunich and Dirk Beuchle for their help during the initial and final phases of the work, respectively. We are also grateful to the Functional Genomics Center Zurich (FGCZ) for support of the MS analyses. The work was supported by the Deutsche Forschungsgemeinschaft (DFG LE 987/5-1).

References

Brand, A. H., Perrimon, N., 1993. Targeted gene expression as a means of altering cell fates and generating dominant phenotypes. Development. 118**,** 401-415.

Brunner, E., Ahrens, C.H., Mohanty, S., Baetschmann, H., Loevenich, S., Potthast, F., Deutsch, E.W., Panse, C., de Lichtenberg, U., Rinner, O., Lee, H., Pedrioli, P.G., Malmstrom, J., Koehler, K., Schrimpf, S., Krijgsveld, J., Kregenow, F., Heck, A.J., Hafen, E., Schlapbach, R., Aebersold, R., 2007. A high-quality catalog of the Drosophila melanogaster proteome. Nat Biotechnol. 25, 576-583.

Buszczak, M., Paterno, S., Lighthouse, D., Bachman, J., Planck, J., Owen, S., Skora, A. D., Nystul, T. G., Ohlstein, B., Allen, A., Wilhelm, J. E., Murphy, T. D., Levis, R. W., Matunis, E., Srivali, N., Hoskins, R. A., Spradling, A. C., 2007. The carnegie protein trap library: a versatile tool for Drosophila developmental studies. Genetics. 175**,** 1505-31.

Cook, H. A., Koppetsch, B. S., Wu, J., Theurkauf, W. E., 2004. The Drosophila SDE3 homolog armitage is required for oskar mRNA silencing and embryonic axis specification. Cell. 116**,** 817-29.

den Elzen, N., Pines, J., 2001. Cyclin A is destroyed in prometaphase and can delay chromosome alignment and anaphase. J Cell Biol. 153**,** 121-36.

Edgar, B. A., Orr-Weaver, T. L., 2001. Endoreplication cell cycles: more for less. Cell. 105**,** 297-306.

Edgar, B. A., Sprenger, F., Duronio, R. J., Leopold, P., O'Farrell, P. H., 1994. Distinct molecular mechanisms regulate cell cycle timing at successive stages of Drosophila embryogenesis. Genes Dev. 8**,** 440-452.

Evans, T., Rosenthal, E. T., Youngblom, J., Distel, D., Hunt, T., 1983. Cyclin: A protein specified by maternal mRNA in sea urchin eggs that is destroyed with each cleavage division. Cell. 33**,** 389-397.

Finley Jr., R. L., Brent, R., 1994. Interaction mating reveals binary and ternary connections between Drosophila cell cycle regulators. Proc. Natl. Acad. Sci. USA. 91**,** 12980-12984.

Finley Jr., R. L., Thomas, B. J., Zipursky, S. L., Brent, R., 1996. Isolation of Drosophila cyclin D, a protein expressed in the morphogenetic furrow before entry into S phase. Proc. Natl. Acad. Sci. USA. 93**,** 3011-3015.

Fischer, M. G., Heeger, S., Hacker, U., Lehner, C. F., 2004. The mitotic arrest in response to hypoxia and of polar bodies during early embryogenesis requires Drosophila Mps1. Curr Biol. 14**,** 2019-24.

Follette, P. J., Duronio, R. J., O'Farrell, P. H., 1998. Fluctuations in cyclin E levels are required for multiple rounds of endocycle S phase in Drosophila. Curr Biol. 8**,** 235-8.

Guo, J., Song, J., Wang, F., Zhang, X. S., 2007. Genome-wide identification and expression analysis of rice cell cycle genes. Plant Mol Biol. 64**,** 349-60.

Hacker, U., Perrimon, N., 1998. DRhoGEF2 encodes a member of the Dbl family of oncogenes and controls cell shape changes during gastrulation in Drosophila. Genes Dev. 12**,** 274-84.

Hagting, A., Karlsson, C., Clute, P., Jackman, M., Pines, J., 1998. MPF localization is controlled by nuclear export. EMBO J. 17**,** 4127-38.

Hatfield, S. D., Shcherbata, H. R., Fischer, K. A., Nakahara, K., Carthew, R. W., Ruohola-Baker, H., 2005. Stem cell division is regulated by the microRNA pathway. Nature. 435**,** 974-8.

Hoskins, R. A., Nelson, C. R., Berman, B. P., Laverty, T. R., George, R. A., Ciesiolka, L., Naeemuddin, M., Arenson, A. D., Durbin, J., David, R. G., Tabor, P. E., Bailey, M. R., DeShazo, D. R., Catanese, J., Mammoser, A., Osoegawa, K., de Jong, P. J.,

Celniker, S. E., Gibbs, R. A., Rubin, G. M., Scherer, S. E., 2000. A BAC-based physical map of the major autosomes of Drosophila melanogaster. Science. 287**,** 2271-4.

Huet, F., Lu, J. T., Myrick, K. V., Baugh, L. R., Crosby, M. A., Gelbart, W. M., 2002. A deletion-generator compound element allows deletion saturation analysis for genomewide phenotypic annotation. Proc Natl Acad Sci U S A. 99**,** 9948-53.

Hwang, H. C., Clurman, B. E., 2005. Cyclin E in normal and neoplastic cell cycles. Oncogene. 24**,** 2776-86.

Jackman, M., Kubota, Y., den Elzen, N., Hagting, A., Pines, J., 2002. Cyclin A- and cyclin E-Cdk complexes shuttle between the nucleus and the cytoplasm. Mol Biol Cell. 13**,** 1030-45.

Jacobs, H. W., Knoblich, J. A., Lehner, C. F., 1998. Drosophila Cyclin B3 is required for female fertility and is dispensable for mitosis like Cyclin B. Genes Dev. 12**,** 3741-51.

Karr, T. L., Alberts, B. M., 1986. Organization of the cytoskeleton in early Drosophila embryos. J Cell Biol. 102**,** 1494-509.

Kerrebrock, A. W., Miyazaki, W. Y., Birnby, D., Orr-Weaver, T. L., 1992. The Drosophila mei-S322 gene promotes sister chromatid cohesion in meiosis following kinetochore differentiation. Genetics. 130**,** 827-841.

Knoblich, J. A., Sauer, K., Jones, L., Richardson, H., Saint, R., Lehner, C. F., 1994. Cyclin E controls S phase progression and its downregulation during Drosophila embryogenesis is required for the arrest of cell proliferation. Cell. 77**,** 107-120.

Kolonin, M. G., Finley, R. L., Jr., 2000. A role for cyclin J in the rapid nuclear division cycles of early Drosophila embryogenesis. Dev Biol. 227**,** 661-72.

Lehner, C. F., O'Farrell, P. H., 1989. Expression and function of Drosophila cyclin A during embryonic cell cycle progression. Cell. 56**,** 957-968.

Lehner, C. F., O'Farrell, P. H., 1990. The roles of Drosophila cyclin A and cyclin B in mitotic control. Cell. 61**,** 535-547.

Lilly, M. A., Spradling, A. C., 1996. The Drosophila endocycle is controlled by cyclin E and lacks a checkpoint ensuring S-phase completion. Genes Dev. 10**,** 2514-2526.

Makarenkov, V., 2001. T-REX: reconstructing and visualizing phylogenetic trees and reticulation networks. Bioinformatics. 17**,** 664-8.

Meyer, C. A., Jacobs, H. W., Datar, S. A., Du, W., Edgar, B. A., Lehner, C. F., 2000. Drosophila Cdk4 is required for normal growth and is dispensable for cell cycle progression. EMBO J. 19**,** 4533-4542.

Morgan, D. O., 2007. The Cell Cycle - Principles of Control. New Sience Press Ltd., London.

Page, A. W., Orr-Weaver, T. L., 1997. Activation of the meiotic divisions in Drosophila oocytes. Dev Biol. 183**,** 195-207.

Page, S. L., Hawley, R. S., 2001. c(3)G encodes a Drosophila synaptonemal complex protein. Genes Dev. 15**,** 3130-43.

Parks, A. L., Cook, K. R., Belvin, M., Dompe, N. A., Fawcett, R., Huppert, K., Tan, L. R., Winter, C. G., Bogart, K. P., Deal, J. E., Deal-Herr, M. E., Grant, D., Marcinko, M., Miyazaki, W. Y., Robertson, S., Shaw, K. J., Tabios, M., Vysotskaia, V., Zhao, L., Andrade, R. S., Edgar, K. A., Howie, E., Killpack, K., Milash, B., Norton, A., Thao, D., Whittaker, K., Winner, M. A., Friedman, L., Margolis, J., Singer, M. A., Kopczynski, C., Curtis, D., Kaufman, T. C., Plowman, G. D., Duyk, G., Francis-Lang, H. L., 2004. Systematic generation of high-resolution deletion coverage of the Drosophila melanogaster genome. Nat Genet. 36**,** 288-92.

Peters, J. M., 2006. The anaphase promoting complex/cyclosome: a machine designed to destroy. Nat Rev Mol Cell Biol. 7**,** 644-56.

Reber, A., Lehner, C. F., Jacobs, H. W., 2006. Terminal mitoses require negative regulation of Fzr/Cdh1 by Cyclin A, preventing premature degradation of mitotic cyclins and String/Cdc25. Development. 133**,** 3201-11.

Sauer, K., Knoblich, J. A., Richardson, H., Lehner, C. F., 1995. Distinct modes of cyclin E/cdc2c kinase regulation and S phase control in mitotic and endoreduplication cycles of Drosophila embryogenesis. Genes Dev. 9**,** 1327-1339.

Schittenhelm, R. B., Heeger, S., Althoff, F., Walter, A., Heidmann, S., Mechtler, K., Lehner, C. F., 2007. Spatial organization of a ubiquitous eukaryotic kinetochore protein network in Drosophila chromosomes. Chromosoma. 116**,** 385-402.

Sigrist, S. J., Lehner, C. F., 1997. Drosophila fizzy-related down-regulates mitotic cyclins and is required for cell proliferation arrest and entry into endocycles. Cell. 90**,** 671-681.

Spradling, A. C., Developmental genetics of oogenesis. In: M. Bate, A. Martinez Arias, Eds.), The development of Drosophila melanogaster, Vol. 1. Cold Spring Harbor Laboratory Press, Cold Spring Harbor, NY, 1993, pp. 1-70.

Sprenger, F., Yakubovich, N., O'Farrell, P. H., 1997. S phase function of Drosophila cyclin A and its downregulation in G1 phase. Curr. Biol. 7**,** 488-499.

Thibault, S. T., Singer, M. A., Miyazaki, W. Y., Milash, B., Dompe, N. A., Singh, C. M., Buchholz, R., Demsky, M., Fawcett, R., Francis-Lang, H. L., Ryner, L., Cheung, L. M., Chong, A., Erickson, C., Fisher, W. W., Greer, K., Hartouni, S. R., Howie, E., Jakkula, L., Joo, D., Killpack, K., Laufer, A., Mazzotta, J., Smith, R. D., Stevens, L. M., Stuber, C., Tan, L. R., Ventura, R., Woo, A., Zakrajsek, I., Zhao, L., Chen, F., Swimmer, C., Kopczynski, C., Duyk, G., Winberg, M. L., Margolis, J., 2004. A complementary transposon tool kit for Drosophila melanogaster using P and piggyBac. Nat Genet. 36**,** 283-7.

Wang, G., Kong, H., Sun, Y., Zhang, X., Zhang, W., Altman, N., DePamphilis, C. W., Ma, H., 2004. Genome-wide analysis of the cyclin family in Arabidopsis and comparative phylogenetic analysis of plant cyclin-like proteins. Plant Physiol. 135**,** 1084-99.

Wang, Z., Lin, H., 2005. The division of Drosophila germline stem cells and their precursors requires a specific cyclin. Curr Biol. 15**,** 328-33.

Weiss, A., Herzig, A., Jacobs, H., Lehner, C. F., 1998. Continuous Cyclin E expression inhibits progression through endoreduplication cycles in Drosophila. Curr. Biol. 8**,** 239-42.

Woo, R. A., Poon, R. Y., 2003. Cyclin-dependent kinases and S phase control in mammalian cells. Cell Cycle. 2**,** 316-24.

Figure legends

Figure 1. Cyclin J homologs in metazoans.

A tree based on predicted amino acid sequences illustrates that Cyclin J homologs are encoded in unicellular flagellate and metazoan genomes. A duplication resulting in Cyclin J (J) and Cyclin J-like (Jl) has occurred in mammals. Apart from Cyclin J sequences, additional cyclins of the A-, B-, D- and E-type families were included. Ag: *Anopheles gambiae*; Dm: *Drosophila melanogaster*; Hs: *Homo sapiens*; Mb: *Monosiga brevicollis*; Mm: *Mus musculus*; Nv: *Nematostella vectensis.*

Figure 2. EGFP-Cyclin J expression during oogenesis.

Ovaries from females with *gEGFP-CycJ III.16* resulting in expression EGFP-Cyclin J under control of the *CycJ* regulatory region were fixed and labelled with a DNA stain. (A) ovariole with early stages of oogenesis (germarium until stage 10). (B) stage 12. (C-E) germarium. (F-H) stage 4. (I-K) germinal vesicle region of a stage 12 oocyte. (L-N) region with metaphase I figure of a mature stage 14 oocyte. Bars in A and B correspond to 30 and 100 μm, respectively. All other bars correspond to 10 μm.

Figure 3. Cyclin J-EGFP levels during oocyte maturation.

Oocytes from *gCycJ-EGFP II.6* females at either stage 12 or stage 14 were analyzed by immunoblotting for the presence of Cyclin J-EGFP using antibodies against GFP (anti-GFP, upper panel). Apart from Cyclin J-EGFP, this antibody detects a second band (see asterisk) which is also observed in control ovaries that do not express GFP (data not shown). An anti-PSTAIR peptide antibody, which reacts predominantly with Cdk1 in *Drosophila* was used as an additional loading control (anti-Cdk1). The number of loaded oocytes is indicated on top of lanes 1-4. The position of molecular weight markers is indicated on the right side.

Figure 4. Cyclin J is a Cdk1 partner.

Panel A: Proteins immunoprecipitated with antibodies against GFP from ovary extracts (E) of either *gcal1-EGFP* (Cal1-EGFP) and *gCycJ-EGFP* (CycJ-EGFP) females were analyzed by immunoblotting with anti-GFP, anti-Cdk1 and anti-Cdk2. Cdk1 but not Cdk2 could be detected in the CycJ-EGFP immunoprecipitates (IP). The long exposures shown for maximal anti-Cdk2 sensitivity reveals some non-specific reactions in the extracts apart from the reaction with Cdk2 (arrowhead). The absence of Cdk1 in the control Cal1-EGFP immunoprecipitate (IP) indicates that the interaction of Cdk1 with CycJ-EGFP is specific. The presence of multiple bands after immunoblotting with anti-GFP presumably reflects proteolytic degradation. The position of molecular weight markers is indicated on the right side. .

Panel B and C: The binding preference of EGFP-Cyclin J and Cyclin J-EGFP for Cdk1-myc or Cdk2-myc was analyzed after coexpression in embryos using the UAS/GAL4 system. Panel B: Extracts of embryos expressing Cdk1-myc and/or Cdk2-myc as indicated above the lanes were analyzed by immunoblotting with anti-myc and anti-PSTAIR (anti-Cdk1) which in *Drosophila* detects almost exclusively Cdk1. Probing with anti-myc demonstrates that Cdk1-myc and Cdk2-myc have a distinct electrophoretic mobility and are expressed at equal levels. Anti-PSTAIR reveals equal loading. Panel C: After coexpression of EGFP-Cyclin J or Cyclin J-EGFP with Cdk1-myc and Cdk2-myc, the former but not the latter was co-immunoprecipitated with antibodies against GFP, as revealed by immunoblotting with anti-myc (α-myc). Moreover, the endogenous Cdk1 but not the endogenous Cdk2 was co-immunoprecipitated as well, as revealed by immunoblotting with either mouse anti-PSTAIR (anti-Cdk1) or rabbit anti-Cdk2. These antibodies also detected the myc-tagged versions. However, the corresponding region is not shown in case of the anti-Cdk2 immunoblot because the reaction with Cdk2-myc was obscured in the immunoprecipitates by a strong

signal caused by commigrating heavy chains from rabbit anti-GFP used for immunoprecipitation.

Figure 5. Cyclin J-EGFP is stable during M and G1 and cannot replace Cyclin A.
Sibling embryos with (*CycA*$^{+}$, A-F) or without (*CycA*$^{-}$, G-L) zygotic Cyclin A expression which either did not express Cyclin J-EGFP (A-C, G-I) or expressed it (D-F, J-L) were collected for 1 hour and aged to the stage where the cells in the dorsal epidermis (above the hatched horizontal lines) are in G1 of cycle 17 and those in the ventral epidermis (below the hatched horizontal line) in G2 or M of cycle 16 during normal development. Progression through mitosis 16 does not occur in *CycA*$^{-}$ embryos and therefore all epidermal cells remain in G2. *prd-GAL4* drives expression on the left of the hatched vertical line in the epidermal regions shown after labelling with antibodies against Cyclin A (CycA), Tubulin (Tub) and a DNA stain (DNA). In contrast to Cyclin A, Cyclin J-EGFP is not degraded during mitosis 16 and G1 of cycle 17. Moreover, Cyclin J-EGFP cannot prevent the cell cycle arrest in G2 of cycle 16 when expressed in *CycA*$^{-}$ embryos. Bar corresponds to 10 μm.

Figure 6. Genetic elimination of Cyclin J.
Panel A: The genomic region with *CycJ* and the neighbouring genes *eIF5B*, *armi*, *CG14971* is illustrated schematically. Start sites and direction of transcription are indicated by arrows. Exons are represented by boxes with black filling indicating coding regions. Flp-mediated recombination between FRT sites present within the transposons *PBAC{RB}e01160* and *P{XP}d0735* (insertion sites indicated by triangles) resulted in the deficiency *Df(3L)AJ14*. Genes deleted by *Df(3L)AJ14* were re-introduced by transgenes (*garmi*, *gCycJ*, *gCG14971*) carrying genomic fragments including the genes *armi*, *CycJ* or *CG14971*, respectively, as indicated by the black horizontal lines. Moreover, the position of additional transposon insertions (*P{wHy}CycJ*^{DG29702} and *PBac{5HPw*$^{+}$*}CycJ*^{A138}) in *CycJ* are indicated by triangles.

Panel B: The presence of the expected Flp/FRT-induced deletion was verified by PCR assays using genomic DNA isolated from flies which were homozygous for *Df(3L)AJ14* (*Df(3L)AJ14*) or carried *Df(3L)AJ14* over a balancer chromosome (*Df(3L)AJ14*/*Bal*). Primer pairs amplifying the recombined hybrid *RB-XP* transposon (*RB-XP*), or fragments from the genes *eIF5B* (*eIF5B*), *armi* (*armi*) or *CG14971* (*CG14971*) were used in parallel reactions. These primers did not amplify products when used without template DNA (no DNA).

Panel C: Genomic DNA was isolated from flies which carried *Df(3L)AJ14, garmi III.8, gCG14971 III.10* either over a balancer chromosome (*ΔCycJ*/*Bal*) or homozygously (*ΔCycJ*). A duplex PCR with primer pairs amplifying fragments from the *armi* and *CycJ* genes confirmed the absence of *CycJ* in the flies homozygous for *Df(3L)AJ14, garmi III.8, gCG14971 III.10*.

Panel D: *Df(3L)AJ14, garmi III.8, gCG14971 III.10* embryos which completely lack maternal and zygotic *CycJ* function were fixed during the syncytial stages and labelled with a DNA stain. Spacing and appearance of nuclei during interphase (inter) and during mitotic pro- (pro), meta- (meta), ana- (ana), and telophase (telo) was observed to be indistinguishable from wild type controls (not shown).

Table 1. Viability and fertility of flies without *CycJ*, *armi* or *CG14971*

Genotype	Viability[a)]	Fertility[b)]	
		Female	Male
w^1	n.d.[c)]	100	100
$CycJ^{DG29702}/CycJ^{DG29702}$	n.d.[d)]	102	n.d.
$CycJ^{DG29702}$/*Df(3L)AJ14*	n.d.[d)]	113	n.d.
$CycJ^{DG29702}$/*Df(3L)Exel6095*	n.d.[d)]	110	n.d.
Df(3L)AJ14/Df(3L)AJ14, garmi III.8, gCG14971 III.10	122	111	140
gCycJ II.41/+; Df(3L)AJ14/Df(3L)AJ14, garmi III.8, gCG14971 III.1	124	115	163
Df(3L)AJ14/Df(3L)AJ14, garmi III.8	114	90	120
Df(3L)AJ14/Df(3L)AJ14	97	0	29

a) Progeny flies with the listed genotypes as well as balanced siblings eclosing from the same cross were counted (n > 300). The fraction of progeny with the listed genotype was calculated and expressed in percent of the fraction predicted in case of full viability.

b) Parallel crosses (3-4 for each genotype) with a fixed number of either test females or test males were crossed with the same number w^1 flies. The total number of progeny was counted and expressed in percent of the number of progeny obtained with the w^1 control crosses (n = 1324).

c) n.d., not determined

d) Although not precisely quantified, the viability appears to be normal.

Althoff et al., Figure 1

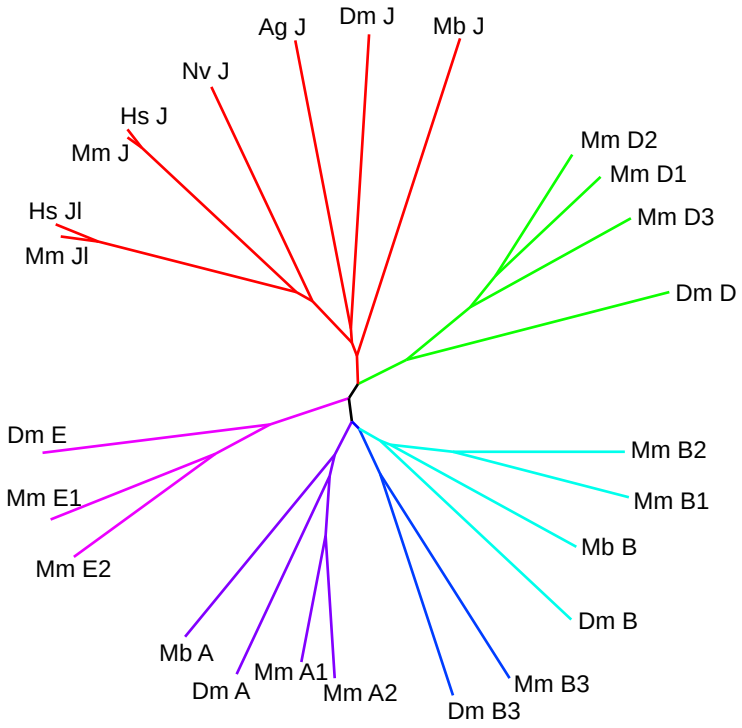

Althoff et al., Figure 2

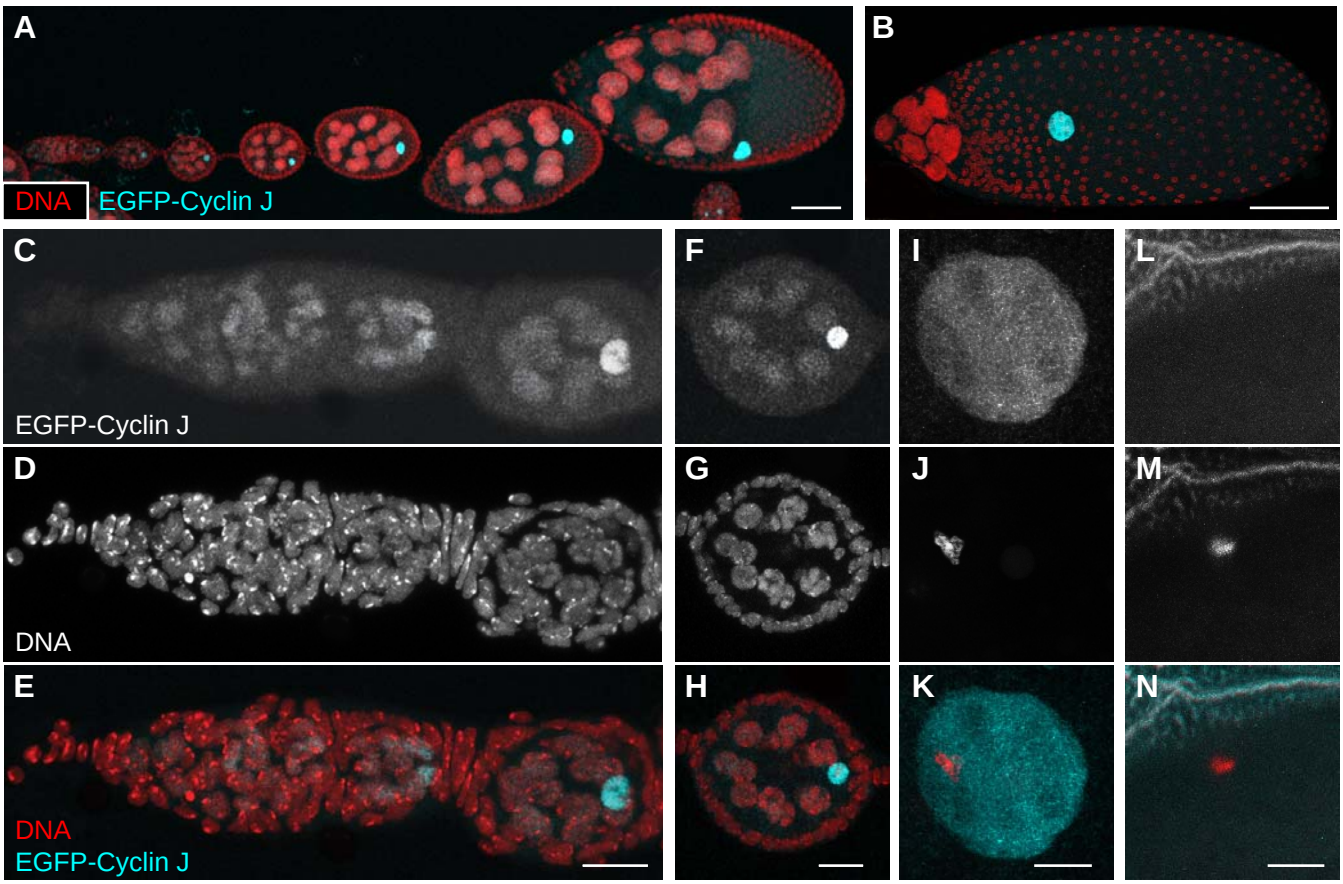

Althoff et al., Figure 3

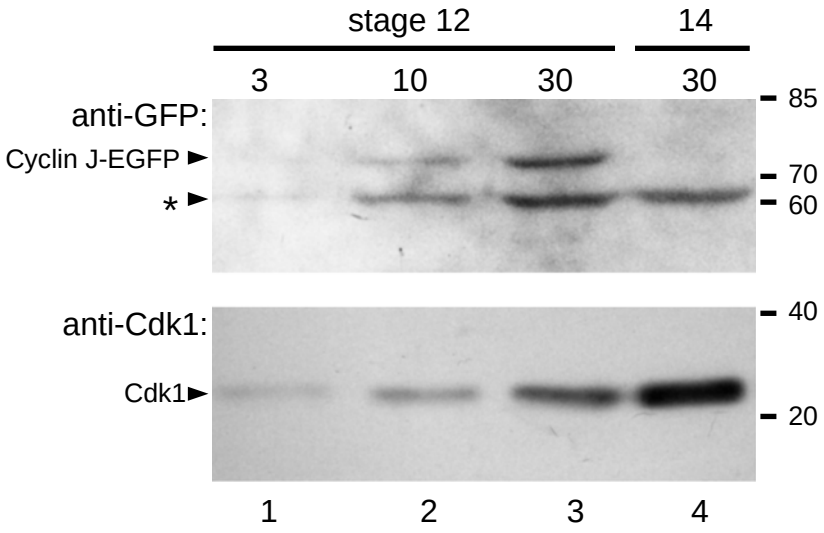

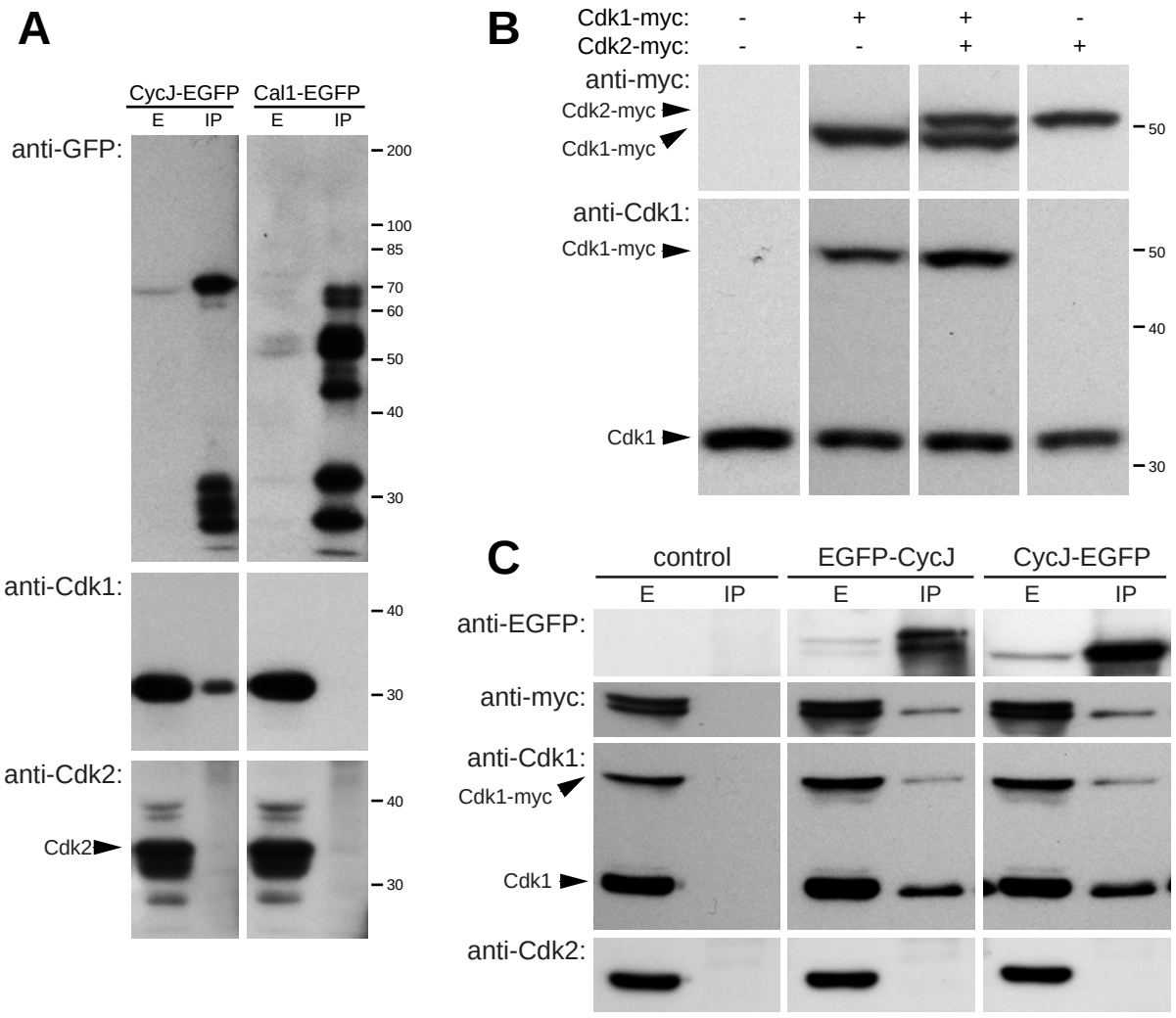
A
CycJ-EGFP
Cal1-EGFP
E
IP
E
IP
anti-GFP:
200
100
85
70
60
50
40
30
anti-Cdk1:
40
30
anti-Cdk2:
Cdk2
40
30
B
Cdk1-myc: - + + -
Cdk2-myc: - - + +
anti-myc:
Cdk2-myc
Cdk1-myc
50
anti-Cdk1:
Cdk1-myc
50
40
Cdk1
30
C
control
EGFP-CycJ
CycJ-EGFP
E
IP
E
IP
E
IP
anti-EGFP:
anti-myc:
anti-Cdk1:
Cdk1-myc
Cdk1
anti-Cdk2:

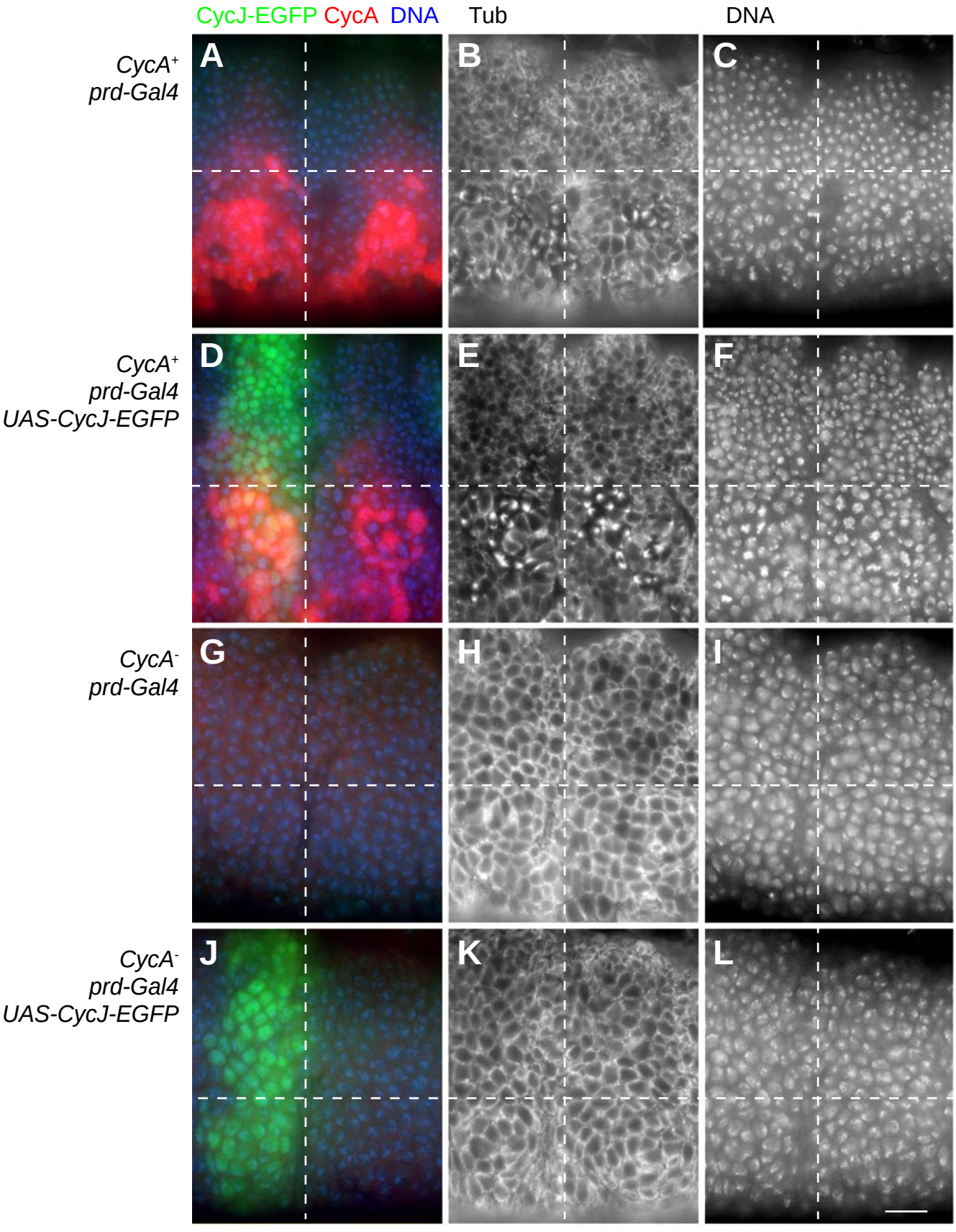
CycJ-EGFP CycA DNA
Tub
DNA
CycA+ prd-Gal4
CycA+ prd-Gal4 UAS-CycJ-EGFP
CycA- prd-Gal4
CycA- prd-Gal4 UAS-CycJ-EGFP
A
B
C
D
E
F
G
H
I
J
K
L

Althoff et al., Figure 6

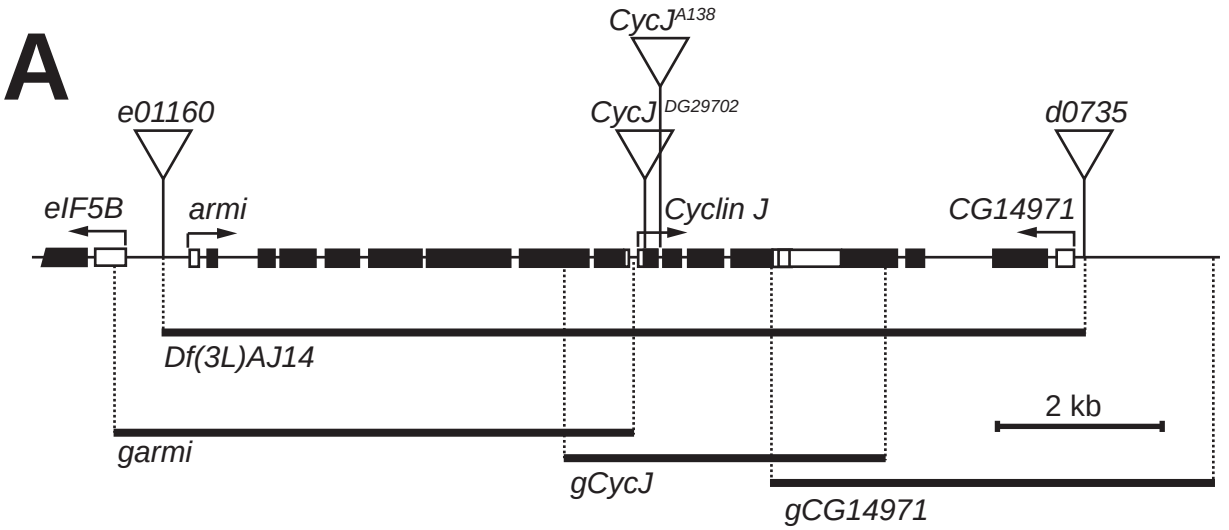

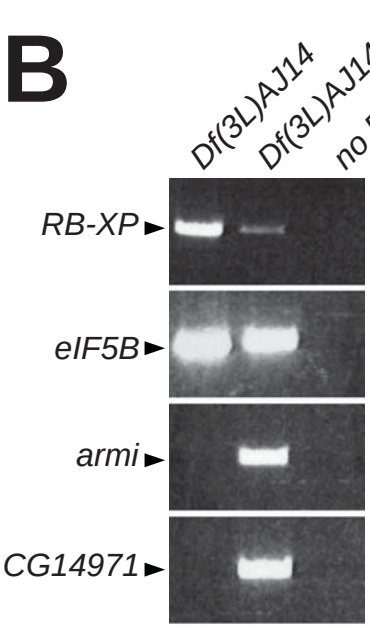

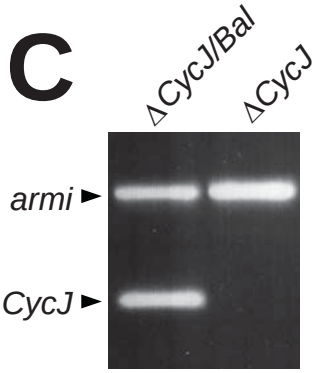

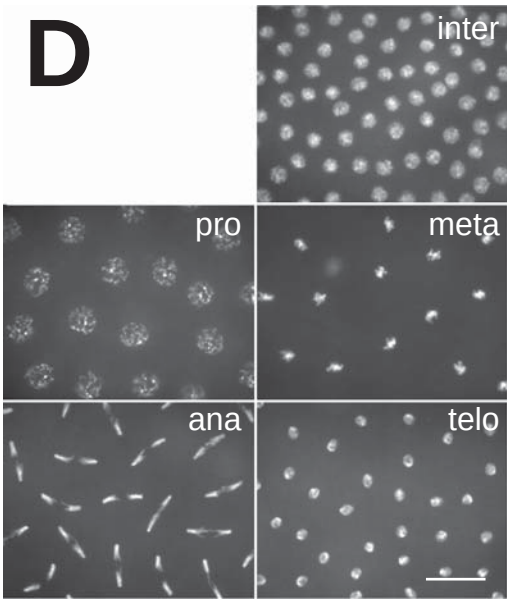

Drosophila Cyclin J is a mitotically stable Cdk1 partner without essential functions

Friederike Althoff[1], Ivana Viktorinová[2], Johanna Kastl[3] and Christian F. Lehner[1,*]

[1] Institute of Zoology, University of Zurich, Zurich, Switzerland

[2] Max-Planck-Institute for Cell Biology and Genetics, Dresden, Germany

[3] Department of Biology, Molecular Genetics, University of Constance, Germany

[*] Correspondence to: Christian F. Lehner, University of Zurich, Institute of Zoology Winterthurerstrasse 190, 8057 Zurich, Switzerland, Tel.: 41 44 63 54871; FAX: 41 44 63 56820; E mail: christian.lehner@zool.uzh.ch

Supplementary Material

- Supplementary Table1.
Proteins co-immunoprecipitated with CycJ-EGFP

- Supplementary Figure 1.
Progression through the syncytial division cycles in *CycJ*-deficient embryos heterozygous for mutations in other cyclin genes

Supplementary Table 1: Proteins co-immunoprecipitated with CycJ-EGFP

Immunoprecipitates isolated with anti-GFP from ovary extracts of either *gCycJ-EGFP II.6* or *gCal1-EGFP II.1* females were resolved by gel electrophoresis. Thereafter the gel lanes were cut from top to bottom into 15 slices, each of which was digested with trypsin before MS/MS analysis of the resulting peptides using the MASCOT search engine (www.matrixscience.com). The table includes all Drosophila proteins for which at least one peptide with either an ion score of >40 or an expect value of $<10^{-4}$ was detected. For each gel slice, the identified proteins are ordered from top to bottom according to the number of different peptides detected with the protein revealed by the maximal number of detected peptides on top. Proteins which were observed in both immunoprecipitates (CycJ-EGFP and Cal1-GFP control) and thus appear to represent non-specifically associated contaminants are marked in green. Cdk1/Cdc2 which is marked in red was only detected in the CycJ-EGFP immunoprecipitate. The other proteins that were only detected in the CycJ-EGFP immunoprecipitate are in general highly abundant proteins (like ribosomal proteins) and some of these have been detected as contaminants in earlier co-immunoprecipitation experiments (unpublished observations). None of these proteins is a protein kinase family member.

region	MW	CG number	name	comment
1	> 270 kD	-		
2	~ 150-270 kD	-		
3	~ 100-150 kD	CG3999		glycine dehydrogenase
		CG2331	TER94	
		CG34333		APAAPSYS repeat protein
4	~ 80-100 kD	CG3999		glycine dehydrogenase
		CG4264	Hsc70-4	
		CG2175	dec-1	
		CG1242	Hsp83	
		CG34333		APAAPSYS repeat protein
		CG4147	Hsc70-3	
		CG8542	Hsc70-5	
		CG7470		aldehyde dehydrogenase family member
5	~ 65-80 kD	CG2175	dec-1	
		CG4246	Hsc70-4	alternatively CG8937(Hsc70-1)
		CG12101	Hsp60	alternatively CG7235 (Hsp60C)
6	~ 52-65 kD	CG2175	dec-1	
		CG9277	βTub56D	
		CG4799	Pen	
		CG3612	blw	
		CG2512	αTub84D	alternatively CG1913 (αTub84B)
		CG9050	Fcp26Aa	
		CG3999		glycine dehydrogenase
		CG8351	Tcp-1η	
		CG1799	ras	
		CG34333		APAAPSYS repeat protein
		CG2985	Yp1	
7	~ 45-52 kD	CG2985	Yp1	
		CG2979	Yp2	
		CG11129	Yp3	
		CG9277	βTub56D	
		CG4027	Act5C	alternatively product of other Actin paralogs
		CG2175	dec-1	
		CG11154	ATPsyn-β	
		CG8280	Ef1α48D	
		CG1489	Pros45	
		CG2152	Pcmt	
		CG34333		APAAPSYS repeat protein
		CG4863	RpL3	
		CG9677	Int6	
		CG3999		glycine dehydrogenase
		CG9124	eIF-3p40	
		CG5502	RpL4	
		CG2098	ferrochelatase	
8	~ 38-45 kD	CG11129	Yp3	
		CG8882	Trip1	
		CG34333		APAAPSYS repeat protein
		CG14792	sta	
		CG9124	eIF-3p40	
		CG7010	l(1)G0334	
		CG2175	dec-1	
9	~ 34-38 kD	CG5363	cdc2	
10	~ 32-34 kD	CG2152	Pcmt	
		CG5363	cdc2	
		CG3999		glycine dehydrogenase
		CG4183	Hsp26	
		CG9769		eIF3f
11	~ 26-32 kD	CG2152	Pcmt	
		CG1633	Jafrac1	
		CG3481	Adh	
12	~ 18-26 kD	-		
13	~ 12-18 kD	CG17949	His2B	
		CG14542		charged multivesicular body protein 2A (ESCRT-III)
		CG34333		APAAPSYS repeat protein
		CG9916	Cyp1	
		CG4464	RpS19a	
		CG4918	RpLP2	
		CG3922	RpS17	
14	~ 8-12 kD	CG3999		glycine dehydrogenase
15	< 8 kD	-		

Supplementary Figure 1: Progression through the syncytial division cycles in *CycJ*-deficient embryos heterozygous for mutations in other cyclin genes

Embryos were collected from females that either had one copy of the *CycJ* gene (*Df(3L)AJ14/+*) or none (*Df(3L)AJ14/ΔCycJ = Df(3L)AJ14, garmi III.8, gCG14971 III.10*). In addition, these females had either two functional copies of other cyclin genes (+/+) or only one functional copy of a particular cyclin gene in trans over a mutant allele ($CycA^{neo114}$/+, $CycA^{C8LR1}$/+, $CycB^{2}$/+, $CycB^{3}$/+, $CycB3^{3}$/+, $CycE^{AR95}$/+, or $CycE^{pz5}$/+). After one hour of egg collection, one half was fixed immediately (red bars) while the other half was aged for an additional hour at 25°C before fixation (blue bars). The embryos were stained with a DNA stain and staged microscopically (n > 200 for each genotype). The bar diagram displays the fraction of embryos which were found to be at a developmental stage either before mitosis 1 (before M1), during cycles 1-4 (1-4), 5-9 (5-9), 10-13 (10-13), interphase 14 (I14), or after onset of mitosis 14 (>M14). The fraction of embryos with abnormal phenotypes like chromatin bridges during anaphase and telophase or irregular spacing of nuclei or mitotic figures was found to be below 3% for all of the analyzed genotypes. The embryos in the aged collections obtained from *CycJ*-deficient females which were before M1 (blue bars marked by asterisks) represent either unfertilized embryos or fertilized embryos which have failed to develop beyond completion of female meiosis. Since their fraction appeared to vary extensively for the different genotypes, we evaluated two additional independent collections and noted a surprisingly poor reproducibility. The average obtained for the three collections (+/- s.d.) is given on the right side. In particular, the high fractions of embryos before M1 observed with some of the *CycJ*-deficient female genotypes (first, second and sixth row from the top) could not be confirmed in these additional experiments.

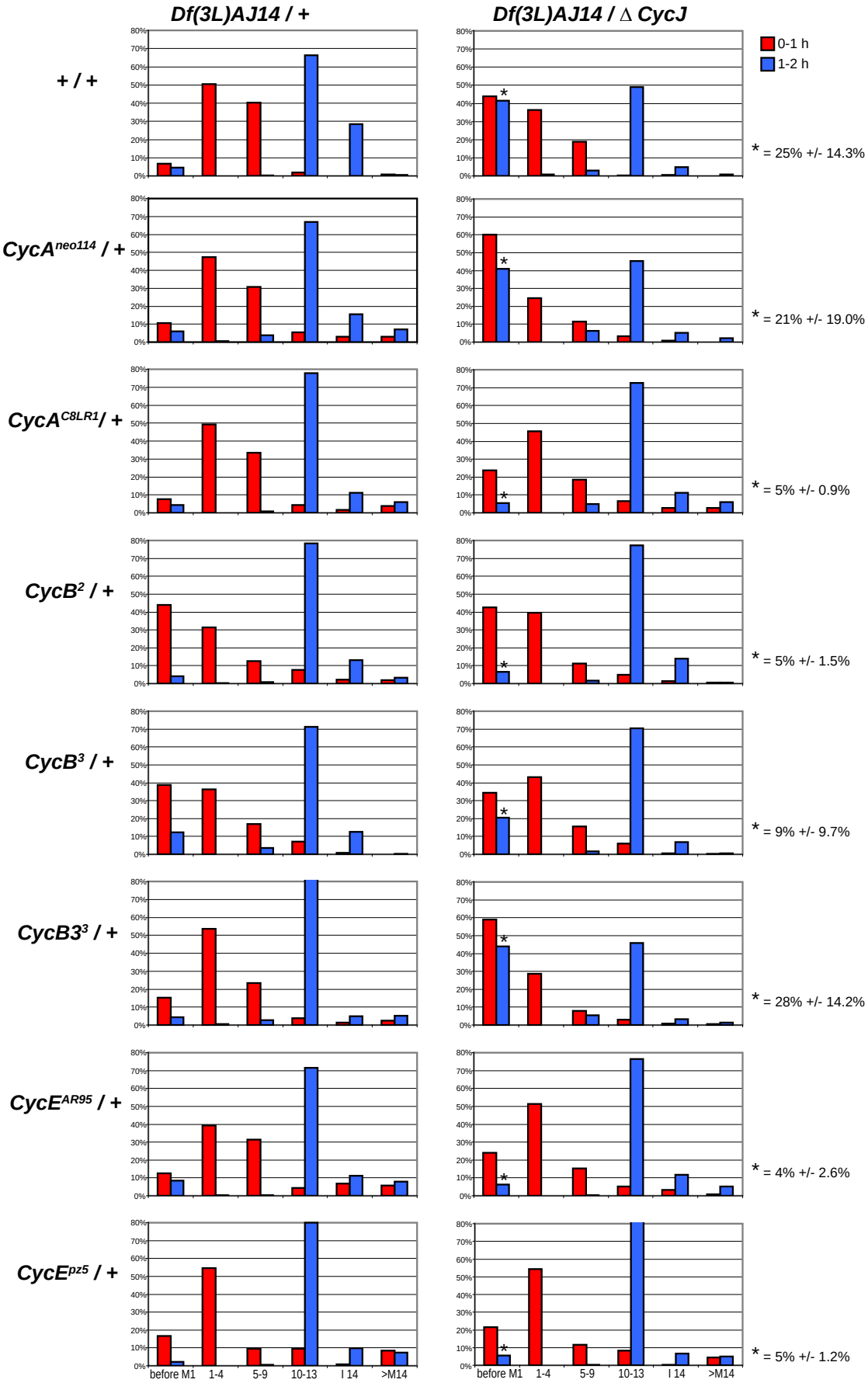
Df(3L)AJ14 / +
Df(3L)AJ14 / Δ CycJ
0-1 h
1-2 h
+ / +
CycA neo114 / +
CycA C8LR1 / +
CycB 2 / +
CycB 3 / +
CycB3 3 / +
CycE AR95 / +
CycE pz5 / +
* = 25% +/- 14.3%
* = 21% +/- 19.0%
* = 5% +/- 0.9%
* = 5% +/- 1.5%
* = 9% +/- 9.7%
* = 28% +/- 14.2%
* = 4% +/- 2.6%
* = 5% +/- 1.2%
before M1
1-4
5-9
10-13
I 14
>M14